Observing the Talbot Effect

Allison Schmitz*

Laser Teaching Center
Department of Physics and Astronomy
Stony Brook University

August, 2003

*NSF-REU Fellow from Austin College, Sherman, Texas.

1 Introduction

In 1836, Henry Fox Talbot, an inventor of photography, made a startling discovery. He found that when he illuminated a periodic grating with a point source of white light he could see colored bands at surprisingly far distances from the grating. These bands alternated between being red and green and being blue and yellow. Talbot himself could not explain the phenomenon; however, about fifty years later, Lord Rayleigh identified it as self-imaging in the Fresnel region. People still investigate and utilize Talbot's discovery today and it has come to be known as self-imaging or the Talbot effect. The imaging of the Talbot effect works similarly to that of a lens; however, there are multiple focal planes behind the grating at which an image may be seen. The distances at which the images occur are found using an equation much like the familiar thin-lens equation:

$$\frac{1}{O} + \frac{1}{I} = \frac{1}{f_n} \tag{1}$$

where

$$f_n = \frac{2na^2}{\lambda} \tag{2}$$

In these equations λ is the wavelength of light, a is the period of the grating, n is any half integer, I is the image distance, O is the object distance, and f_n is a focal length.

When using a point source of divergent light, the distance between each image increases as the observation point moves farther away from the grating, and there is a finite region of focal planes within which the images appear. The Talbot effect can also be observed using parallel light directed through a periodic grating. In this case, the images are spaced evenly at a distance $T_L = \frac{a^2}{\lambda}$ apart. T_L is called the Talbot length, and is the same as the focal length for $n = 1/2$ in the previous equation.

In order to explore these concepts further, I did an experiment consisting of three parts. I first used divergent light to find the image distance for a particular object distance, then I compared the image distance values for multiple object distances, and finally I observed the Talbot effect for parallel light.

2 Experimental set up and procedure

The experimental setup consisted of a helium-neon laser with $\lambda = 632.8$ nm, a 2×2 inch Ronchi grating with 250 lines/inch (Edmund Scientific, model NT56-609), an Electrim 1000N CCD camera, and a Gaertner 1.2 m precision optical bench with various carriages. The laser was coupled through a single-mode fiber optic cable to provide a convenient point source of divergent light. The end of the fiber, the grating, and the CCD camera were each mounted on to separate carriages. The light from the fiber was directed at the grating, where it was diffracted towards the camera. Images were stored and viewed with the Electrim imaging software included with the camera. The optical bench has a ruler that measures millimeters and the carriages each have a ruler that has nine marks for every 10 millimeters. Therefore the bench measures intervals as small as 100 microns.

I first used Equation 1 to predict where images would occur for one particular value for the object distance, and then I moved the camera back in 1 mm intervals, noting the positions at which images occurred. As the camera was moved back, I took pictures at each step, which were saved for later analysis. I used 3 of these pictures, one at the first observable Talbot image, one at the last, and one at a point in between two images, to make intensity plots. For the second part of this experiment, I compared the image distance values for multiple object distances, following the same procedure as I did for the first part. The third part of my experiment has a slightly different set up. In this case, a plano-convex lens was placed between the fiber and the grating, so that the diverging laser light was collimated (made parallel) before passing through the grating. I observed several images and compared their separation with the Talbot length T_L defined above.

3 Results

The results from all of the experiments using a point source of light are summarized in Table 1. This shows, for each of five different object distances, the predicted value for the image distance as well as an average experimental value. It is apparent that as the object distance increases the images move closer together, so that there are more focal planes for larger object distances.

The missing entries in the table can be due to one of three things. First, because of the size of the carriages, the camera could only get within $\sim$5 cm of the grating, so that any image that occurred before this position could not be viewed. In addition, the overall length of the optical bench limited the distance to which the images could be measured to $\sim$90 cm. Finally, the total number of possible images is limited in any case by the relation $f_n < O$ that follows from Equation 1. For example, for an object distance of $O = 13$ cm, the maximum value of n is 3.5, since the Talbot length $T_L = \frac{a^2}{\lambda} = 1.631$ cm.

To illustrate how the image distance changes for a sequence of focal planes, I used the theoretical and experimental data for an object distance of $O = 13$ cm to make the graph in Figure 1. In the graph, the x's represent the theoretical predictions, and the lines represent the experimental values. There are error bars around the experimental values indicating the range in which the measurements lie. It can be seen that the observations are all in very good agreement with the predictions.

In Figure 2, I have plotted the inverse of the image distance versus the inverse of the object distance for several values of n to illustrate the linear relationship implied by Equation 1. In this linear relationship, the x and y intercepts are both equal to the reciprocal of the focal length, f_n^{-1}, and the slope is negative one. In the figure the four lines at successively larger distances from the origin correspond to n values of 3, 2.5, 2 and 1.5, respectively. The points correspond to the experimental observations, which are seen to be in excellent agreement with the predicted lines.

I also converted several of the images taken with the CCD camera at an object distance of $O = 13$ cm into an intensity profile, as shown in the three plots in Figure 3. At camera distances corresponding to a specific image distance, the plot is very ordered, and resembles the original Ronchi grating pattern. The first (top) plot in Figure 3 is for $I = 8.0$ cm while the next (middle) plot is of the fourth and last image at $I = 40.9$ cm from the grating.

The same order that is seen in the plot of the first image is evident in this one as well, but now there are fewer bars. This occurs because the image becomes magnified as the image distance increases. The third plot in Figure 3 (bottom) corresponds to a distance between two images. This plot is disordered, unlike the other two. In fact, at the points in between Talbot images, the pattern is highly complex; fractal.

As can be seen from the intensity plots in Figure 3, the Talbot images magnify as the distance from the grating increases. The magnification can be found using the same formula that applies to a normal lens:

$$M = \frac{I + O}{O} \tag{3}$$

The predicted and observed values of the magnification are in good agreement, as summarized in Table 2.

Finally, I used the same setup to observe the Talbot effect for parallel light. Since the Talbot length is $T_L = 1.631$ cm, the images of the grating should occur regularly at this interval. In actual observation, the images occurred slightly further apart, every 1.7 cm. This discrepancy might have been caused by the lens being at not quite the correct distance from the point source, so that the light wasn't perfectly collimated. The images also all had the same magnification ($M = 1$), as expected.

4 Conclusions

My observations were in quite good agreement with theory in nearly every case. Using a point source of light, the interval between focal planes increases as the image distance increases, while when using parallel light the interval remains constant. Also, when using a point source, as the object distance increases, the focal planes become closer together so that there are more of them.

One difficulty I encountered in observing the images was interference fringes. A reflection from the front of the Ronchi grating interferes with a reflection from the back of the grating, so that circular fringes appear on top of the image. This makes it difficult to see the image; however, when using the CCD camera, the Talbot lines are more obvious than the interference fringes. It was also difficult to get a clear plot of the intensity. In the plots shown in Figure 3, the lines are slightly jagged instead of being perfectly straight. This occurs because it was difficult to keep the Ronchi grating straight, that is, parallel to the pixels of the CCD camera. Also, the image may not be perfectly in focus since the camera was moved in 1 mm steps.

All in all, however, the measurements are quite accurate because of the very precise optical bench. In Figure 1, the graph of image distance versus n with error bars, the theoretical predictions are within the error range of ± 0.5 mm. The only significant discrepancy in any of the measurements was in the Talbot length measured with parallel light. This relatively large error (4.3 %) was most likely due to the light not being correctly focused.

The Talbot effect is related to many diverse phenomena in mathematics and theoretical physics. For example, "quantum revivals" are analogous to the Talbot effect. The wave

packet corresponding to a particle begins its order in a particular form and returns to that form periodically. In mathematics, the Talbot effect is related to "fractal carpets." At points at which the Talbot distance is multiplied by an irrational fraction, the intensity plot is fractal, as shown in Figure 3. The Talbot effect is also related to number theory. When the Talbot distance is multiplied by $\frac{p}{q}$, where are p and q are integers, there are q superimposed images of the grating. Finally, the Talbot effect has many interesting and useful applications to both classical and atom optics. For example, the effect can be used to focus atom beams, and it is also used in some spectrometer designs.

In the future, I plan to try to simulate the Talbot effect on a computer to better understand why it occurs. This shouldn't be too difficult if the Ronchi grating is approximated by one with a relatively small number of narrow slits.

Acknowledgements

I would like to express my gratitude to Dr. John Noé and Professor Harold Metcalf for all of their support in the Laser Teaching Center. I am also grateful to Professor Erlend Graf for the opportunity to participate in the REU program this summer.

References

Ambrosini D. and G. Schirripa Spagnolo. "Talbot effect application: measurement of a distance with a Fourier-transform method" Meas. Science & Technol. **11** (2000): 77-82.

Benko, Zsolt, Margit Hilbert, Zsolt Bor. "New considerations on Talbot's bands" American Journal of Physics **68** (2000): 513-520.

Banaszek, Konrad, Krzysztof Wodkiewicz. "Fractional Talbot effect in phase space: A compact summation formula" Optics Express **2** (1998):169-172.

Berry, Michael, Irene Marzoli, Wolfgang Schleich. "Quantum carpets, carpets of light" Physics Web. June 2001. *physicsweb.org/article/world/14/6/7/1/pw140607fp.*

Bhatnagar, Aparna, Helen L. Kung, David A. B. Miller. "Transform spectrometer based on measuring the periodicity of Talbot self-images" Optics Letters **26** (2001):1645-1647.

Clauser, J.F. "New Theoretical and Experimental Results in Fresnel Optics with Applications to Matter-Wave and X-Ray Interferometry" Applied Physics B **54** (1992): 380-395.

Davis, Christopher C., Igor I. Smolyaninov. "Apparent superresolution in near-field optical imaging of periodic gratings" Optical Society of America **23** (1998):1346-1347.

Furlan, Walter D., Genaro Saavedra, Sergio Granieri. "Simultaneous display of all the Fresnel diffraction patterns of one-dimensional apertures" American Journal of Physics **69** (2001): 799-802.

Givens, M. Parker. "Talbot's bands" American Journal of Physics **61** (1993): 601-605.

Silverman, Mark P. *Waves and Grains: Reflections on Light and Learning.* Princeton: Princeton University Press, 1998.

Image Distances (cm) for Specified Object Distances										
	O=13 cm		**O=15 cm**		**O=17 cm**		**O=19 cm**		**O=21 cm**	
n	pred	exp	pred	exp	pred	exp	pred	exp	pred	exp
0.5	1.86	–	1.83	–	1.80	–	1.78	–	1.77	–
1.0	4.36	–	4.17	–	4.04	–	3.94	–	3.86	–
1.5	7.85	7.89	7.26	7.20	6.87	6.90	6.59	6.60	6.38	6.36
2.0	13.10	13.33	11.50	11.53	10.60	10.64	9.94	9.98	9.47	9.45
2.5	21.89	22.06	17.86	17.98	15.70	15.80	14.30	14.35	13.33	13.40
3.0	39.60	40.44	28.13	28.43	23.10	23.30	20.20	20.35	18.33	18.48
3.5	93.88	–	47.76	48.65	34.80	35.20	28.60	28.89	25.03	25.2
4.0	–	–	100.1	–	56.20	57.15	41.70	42.08	34.47	34.78
4.5	–	–	680.8	–	107.6	–	64.60	65.55	48.79	49.35
5.0	–	–	–	–	–	–	115.3	–	73.08	74.10
5.5	–	–	–	–	–	–	322.8	–	123.3	–

Table 1: Predicted and experimental image distances (cm) for varying object distances

Image Magnifications for O = 13 cm		
n	**pred**	**exp**
1.5	1.60	1.64
2.0	2.01	2.06
2.5	2.68	2.54
3.0	4.05	3.70

Table 2. Predicted and experimental values for the image magnification at an object distance of 13.0 cm.

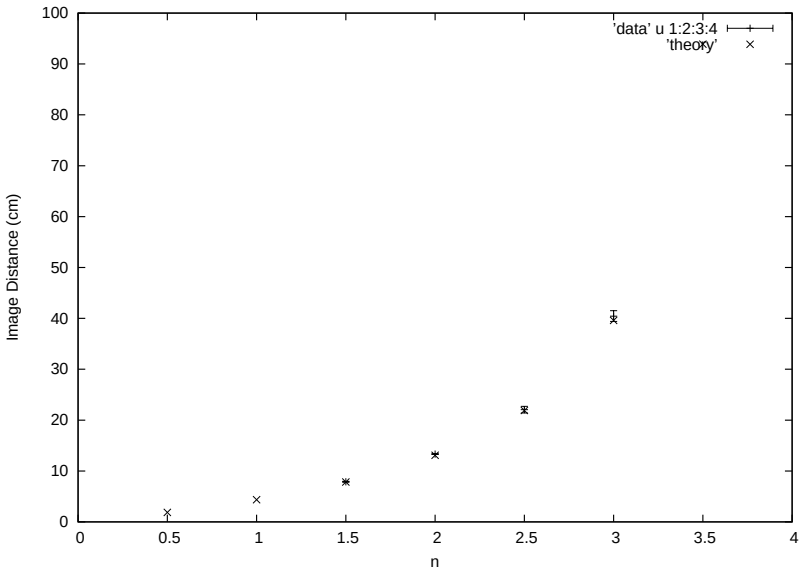

Figure 1. Graph of image distance *versus* n for an object distance of $O = 13$ cm.

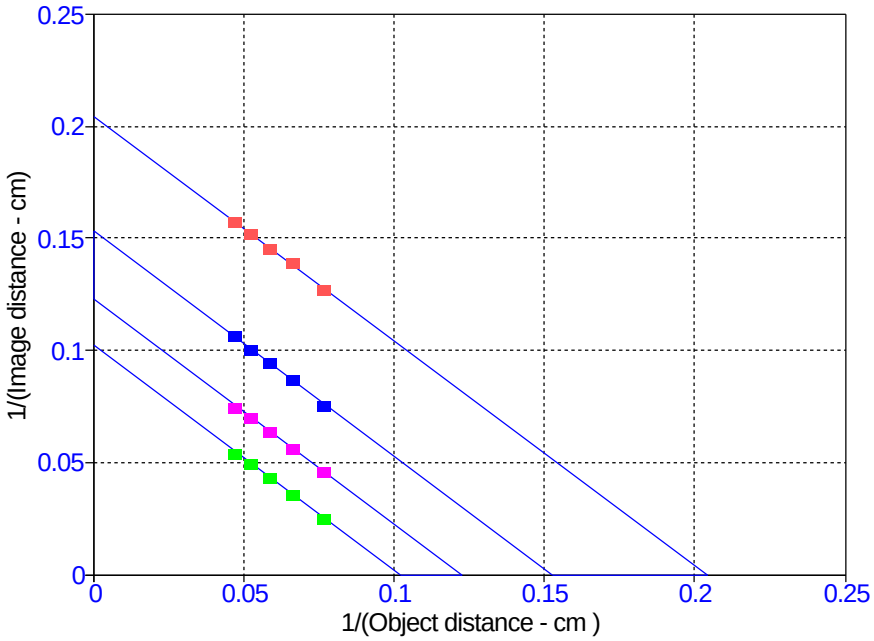

Figure 2. Graph of reciprocal image distance *versus* reciprocal object distance. The four lines at successively larger distances from the origin correspond to n values of 3, 2.5, 2 and 1.5, respectively. The experimental observations (points) are in excellent agreement with the predicted lines.

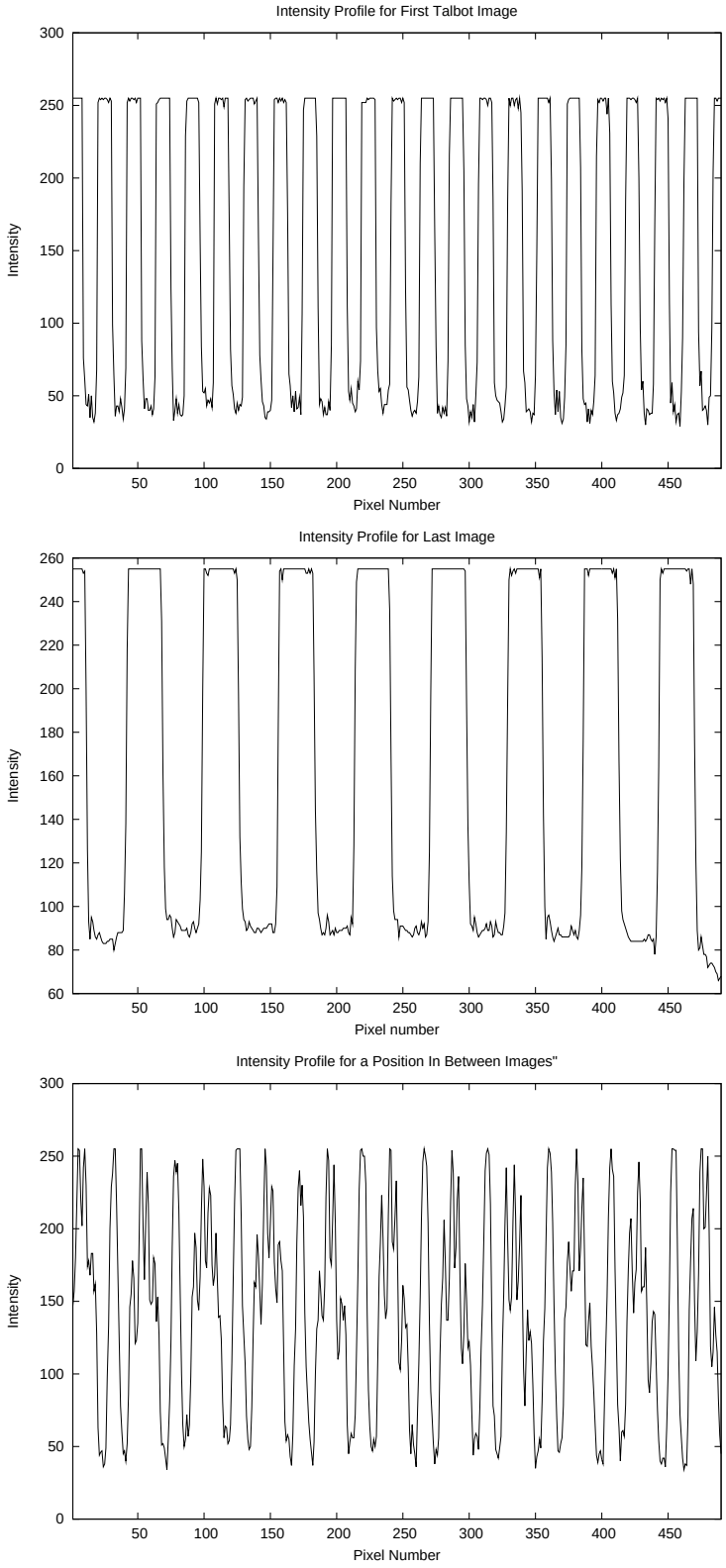

Figure 3. Intensity plots at the first observed image, last observed image, and a point in between two images, respectively. The object distance is 13 cm.